conjunction with the MLC and (3) the patient/phantom. Once the phase-space data of a given accelerator configuration are commissioned, there is no need to perform the simulation through the patient-independent portion of the treatment head again.

2.2.1. Linear accelerator treatment head modelling. The MC treatment head model of our Varian Clinac 2300C/D for a 15 MV photon beam was developed using originally written EGS4 codes. The treatment head was divided into the patient-independent (including target/backing, primary collimator, vacuum window, flattening filter, monitor chamber and mirror) and the patient-dependent (including upper and lower jaws) portions for MC simulation. Respective codes were developed for particle transport through such treatment head components. Each of the treatment head components was modelled in detail on the basis of the specifications for geometry and material compositions provided by the manufacturer. For example, the target/backing was modelled as a two-layer slab with a cylindrical outer boundary. The complex flattening filter model was developed with an arbitrary number of sets of layers and truncated conical sections.

Several errors in the manufacturer's specification have been reported (Bieda *et al* 2001, Sheikh-Bagheri and Rogers 2002). The vagueness of the material specifications is also a matter of concern, as discussed by Siebers *et al* (2005). We have carefully checked the reliability of specifications on the basis of further communication with Varian (Johnsen and Siebers 2005) and the data used in the MC model developed at Virginia Commonwealth University (Keall *et al* 2003, Siebers and Keall 2005). Material compositions and densities were set to match those corresponding to the material specifications that the vendor provides to the part manufacturer. These specifications differ slightly from the pure tungsten used for the target, primary collimator, flattening filter and jaw materials. In the MC simulation, the first phase-space data (PS_1) are scored at the end of the patient-independent portion and then used as an input to the subsequent transport through the patient-dependent portion of the treatment head and the MLC. Approximately 5×10^7 incident electrons were simulated to obtain a total of 2.8×10^8 particles in the PS_1 file on a 28-CPU Linux cluster.

Characteristics of the incident electron beam are poorly specified by the manufacturers; however, many investigators have obtained good agreement with measurements for the Varian machines using electron beam models, of which energy and radial spread are Gaussian in shape (Ding 2002a, Sheikh-Bagheri and Rogers 2002, Keall *et al* 2003, Cho *et al* 2005). For this study, the Gaussian distributions are used to model the incident electron energy and radial intensity spread based upon their previously published works. In the commissioning of the phase-space data, the mean electron energy on target and the FWHM of the radial intensity distribution are the only adjustable simulation parameters. The FWHM of the energy distribution is defined as 3% and the electron beam is perpendicularly incident upon the target with no divergence. In the version of EGS4 used in this study, a bremsstrahlung photon is deflected by a fixed angle and this approximation will cause significant errors in the angular distribution. To improve bremsstrahlung angular sampling, we have employed an extension by Bielajew *et al* (1989) as well as EGSnrc (Kawrakow and Rogers 2003). The variance reduction technique for bremsstrahlung splitting was used to reduce the computation time, and each bremsstrahlung photon was split into 20 photons with a reduced statistical weight. Note that this is the only variance reduction technique used in MCRTV in order to compute doses as accurately as possible.

2.2.2. MLC modelling and dynamic IMRT simulation. The MC model of the Varian Mark II 80-leaf MLC has been developed with originally written EGS4 codes as a part of the patient-dependent portion. Its complex geometry of the tongue-and-groove design, the rounded leaf

tip, and the tapered shape of the leaves were incorporated into the model in great detail based on the machine drawings provided by the manufacturer. Each leaf model consists of a set of sub-regions divided by planes in the x-, y- and z-directions. The rounded leaf tip is modelled with a series of planes inclined according to the actual design. In the y-direction (i.e., perpendicular to leaf motion), the leaf edges are modelled as the planes parallel to the beam ray line from the target. The material composition of each region corresponding to leaf or interleaf air gap is assigned to leaf material or air, respectively. The simulation through the patient-dependent portion is implemented using the PS_1, and the second phase-space data (PS_2) are then obtained under the MLC. The PS_2 is finally used for the simulation in a patient/phantom geometry.

MCRTV is capable of simulating a static MLC field and a dynamic IMRT field. The positions of the leaves are read from a .mlc file created by Eclipse or the MLC field generator (Shaper, Varian Medical Systems, Palo Alto, CA, USA), which specifies the projection of the MLC light field to the isocentre plane. To determine the physical leaf positions, the parameters in the mlctable.txt file provided by Varian are used. The dynamic motion of the MLC leaves is simulated by sampling the leaf positions for each incident history using a cumulative probability distribution function of each leaf position, which can be created from a relationship between the fractional number of monitor units (MUs) and the corresponding leaf positions specified in the .mlc leaf sequence file. A similar method was employed by Liu *et al* (2001) for the DMLCQ component module in the EGS4/BEAM code.

2.2.3. CT-based patient modelling. For the in-patient MC dose calculation, treatment planning CT images are used to develop a voxel-based patient model. The conversion process of CT data to an MC model (i.e., materials and densities) is performed semi-automatically using a program originally developed for MCRTV, which is one of the important features of the GUI application to be discussed below. At first, the CT data are converted to the materials based upon the specific CT number thresholds for each material. We use three tissues (i.e., adipose, soft tissue and bone) and air, and the tissue compositions are obtained from the ICRU report (ICRU 1989). Our program allows adjustment of the CT number thresholds with visual checking as to whether the appropriate material is assigned for each voxel. Once the tissue type is determined for each voxel, the CT data are then converted to the mass density using the CT scanner calibration curve (for the CT number to electron density conversion) and the tissue-specific conversion factor, which is defined as the ratio of the mass density to the electron density for each tissue (for the electron density to mass density conversion). The relationship between the mass density and the electron density is assumed to be linear for each tissue (Brooks *et al* 1981). Table 1 shows composition breakdown and conversion factors of electron density to mass density for the three types of tissues. An MC patient model consists of an arbitrary number of voxels with the uniform x-, y- and z-dimensions ranging from 1 mm to 5 mm. In the MCRTV system, the voxel dimension is set to the value identical to the calculation grid size used in the Eclipse TPS by default. The MC calculated dose is given as the dose to the material (not converted to the dose to water) in the voxel.

2.2.4. Parallel computing. All the MC simulations in MCRTV run on a Linux cluster (Hyper Blade, Appro International, Milpitas, CA, USA), consisting of 14 nodes (2 CPUs/node) of 3.2 GHz Intel Xeon processors. The MC codes have been parallelized using the message passing interface (MPI) for interprocessor communication. Although parallel computing is a meaningful way to reduce the computation time, its accuracy is critically influenced by the quality of the random number generator used. We have implemented the scalable parallel random number generator (SPRNG) (http://sprng.cs.fsu.edu/) in our EGS4 MC codes. Tyagi

Table 1. Composition breakdown (taken from the ICRU reports) and conversion factors of electron density to mass density for the three types of tissues used to build an MC patient model in MCRTV.

Material	Adipose	Soft tissue	Bone
Conversion factor (10^{-26} kg)	0.299	0.302	0.322
H	11.4	10.1	3.4
C	59.8	11.1	15.5
N	0.7	2.6	4.2
O	27.8	76.2	43.5
Na	0.1		0.1
Mg			0.2
P			10.3
S	0.1		0.3
Cl	0.1		
K			
Ca			22.5
Ar			

et al (2004) also used SPRNG in order to parallelize the DPM codes (Sempau *et al* 2000) and obtained excellent agreement between the results computed with serial and parallel code. A simplified description of the parallel computing in MCRTV is shown in figure 2. First, the independent PS_1 data (scored at the end of the patient-independent portion) are calculated for each processor (figure 2(a)), which is performed only during the beam commissioning process, as discussed above. In the usual dose computations for clinical treatment plan verification, we perform the MC simulation only downstream of the patient-independent portion using the well-commissioned PS_1 data (containing a total of 2×10^8 particles) as an input (figure 2(b)). The PS_2 data are created for each processor with a simulation through the patient-dependent portion, which is then used to perform the in-patient/phantom calculation. The results are finally gathered and summed up in the processor with MYRANK = 0, and are then transferred to the GUI application terminal for subsequent processing (see figure 1).

2.2.5. MC calculation parameters and statistical analysis. The EGS4 transport parameters are set to ECUT = AE = 0.70 MeV for electrons and PCUT = AP = 0.010 MeV for photons in all the simulations of MCRTV. To precisely estimate the statistical uncertainty for the in-patient/phantom dose computation, the history-by-history method (Walters *et al* 2002) is employed instead of the ordinary batch approach. In the simulation through the patient-independent portion of the treatment head, each of the scored particles has been tagged with the number of the primary history (incident electron) that generated it. The tag is recorded as the phase-space information and preserved through the simulation to keep track of the relationship between the primary history and the scored particle. For the patient/phantom simulation, the statistical uncertainties are calculated on the basis of the history-by-history method and the output file provides the dose value with its statistical uncertainty (1σ) for each voxel. The MC calculated results are given in absolute dose per MU (cGy MU^{-1}) converted from dose per source particle using the same method as in Siebers *et al* (1999). An empirical correction to account for backscatter to the monitor chambers from the jaws has been performed on the basis of the technique reported by Liu *et al* (2000).

2.3. A GUI application

A GUI application has been originally developed for the clinical application of MCRTV using C++ Builder (Borland, Cupertino, CA, USA) and OpenGL. The GUI has some capabilities

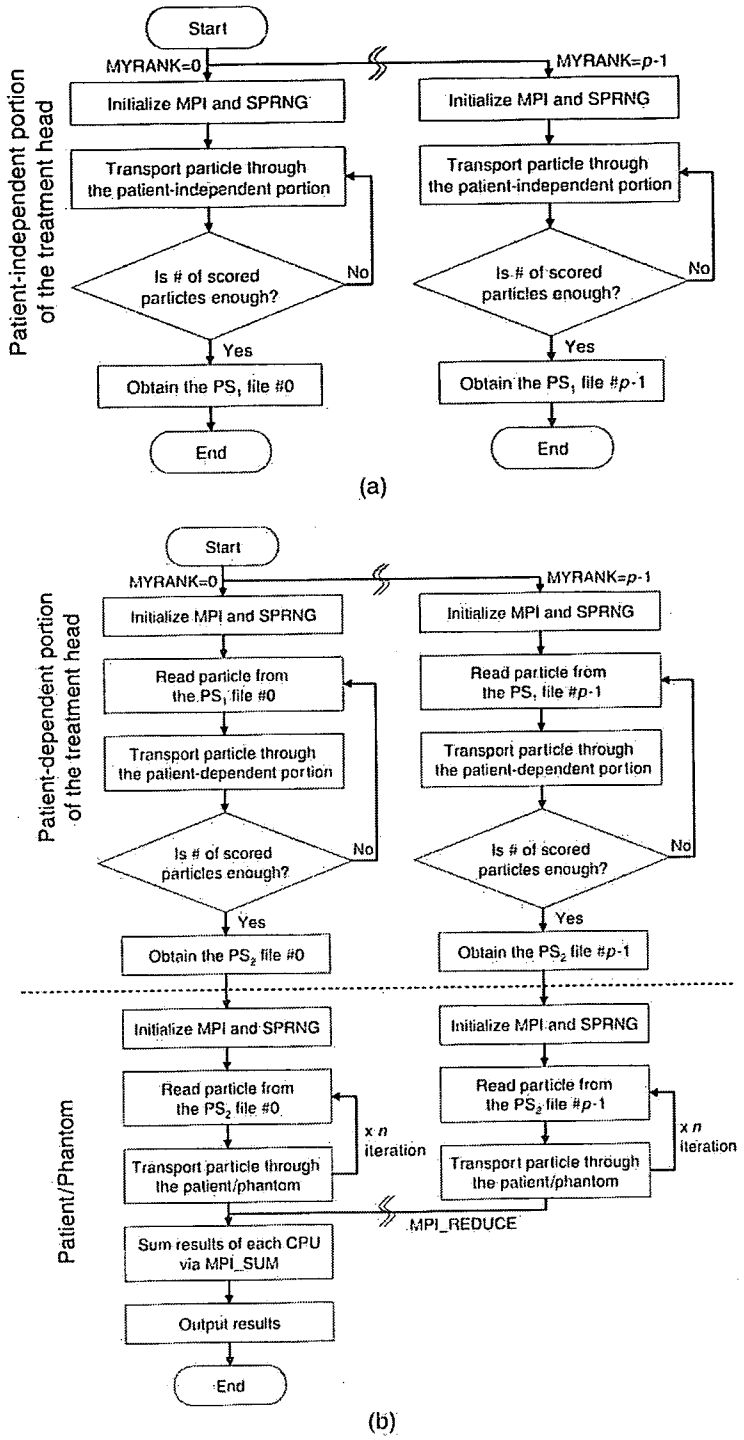

Figure 2. Flow diagrams of the parallel computing for (a) the patient-independent portion of the treatment head and (b) the patient-dependent portion and the patient/phantom. 'MYRANK' is a unique identification number for each processor used in the MPI parallel computing. The total number of processors is indicated by 'p'.

as follows: (1) semiauto-creation of MC input files (i.e., MC patient model and beam configuration), (2) auto-run of the MC simulation, and (3) display and analysis of the MC calculation results. The information needed for MC computation and subsequent process (including the CT image data, the structure data, the plan data and the dose data) are transferred via the interface between MCRTV and Eclipse in DICOM-RT format. An MC patient model (i.e., materials and densities) can be built from the CT data and the CT number thresholds for each material type specified by the user, as discussed in the previous section. An MC input file related to the beam configurations is created automatically from the plan data, which contains field size, gantry angle, couch angle and MLC leaf positions. The input files are transferred to the Linux cluster and the MC simulation is run automatically. For the processing of the MC calculated results, isodose curves are displayed, and the dose volume histograms (DVHs) for the target and the organs at risks (OARs) are calculated using the structure datasets. The calculation results obtained by MC and Eclipse (taken as the dose data) can be compared on the GUI.

2.4. Accuracy benchmarks under homogeneous and inhomogeneous conditions

The accuracy of MCRTV was benchmarked under homogeneous and inhomogeneous conditions in comparison with the measurements and the EGS4/DOSXYZ (Ma *et al* 1995) calculated results. For the benchmarks under the homogeneous condition, the depth dose and the dose profile curves were determined for 6 cm × 6 cm, 10 cm × 10 cm and 20 cm × 20 cm open fields in a 40 cm × 40 cm × 40 cm water phantom (Wellhöfer Blue Phantom, Scanditronix, Uppsala, Sweden) at 100 cm SSD. The respective PS_2 files contained 1×10^7, 3×10^7 and 1×10^8 particles, and they were recycled 20 times in the phantom simulation. The number of particles in the PS_2 files and the number of recycle were determined by investigating the statistics of the MC results for several combinations of those numbers. We found no obvious differences in the statistics between the combinations as well as the results by Walters *et al* (2002). The voxel x-dimension used in the MC calculation was set to 0.5–2 cm (according to the field size) near the field centre, and 0.25 cm on the penumbral region and outside the field to obtain the profiles at a high resolution. Both of the y- and z-dimensions were 0.5 cm. Measurements were performed using the CC-13 ionization chamber (Scanditronix Wellhöfer, Schwarzenbruck, Germany). The effective point of measurement for the ion chamber was taken into account by shifting the measured depth dose curves by $0.6r$ (where r is the radius of the ion chamber cavity). An iterative process, similar to that used by other investigators (Lovelock *et al* 1995, Liu *et al* 1997, Fix *et al* 2001b, Hartmann Siantar *et al* 2001, Ding *et al* 2002a, Sheikh-Bagheri and Rogers 2002, Chetty *et al* 2003, Keall *et al* 2003, Verhaegen and Seuntjens 2003, Cho *et al* 2005) was used to commission the phase-space data. The mean energy and the FWHM of the intensity distribution of the incident electron beam were adjusted so that the resulting depth dose and the dose profile curves in water gave the best match with the measurements. Note that the matching process for the depth dose curves was based on the discrepancies between the MC and the measurements from 5 to 30 cm depths excluding the build-up region. The surface was excluded to avoid the effects of electronic disequilibrium, and there has been a lot of debate on the build-up region discrepancies (Hartmann Siantar *et al* 2001, Ding 2002a, 2002b, Keall *et al* 2003, Abdel-Rahman *et al* 2005). For the dose profile curves, the discrepancies from 0 to 1.5, 3.5 and 8.5 cm off-axis positions were considered for 6 cm × 6 cm, 10 cm × 10 cm and 20 cm × 20 cm open fields, respectively to ensure that the comparisons were in the umbral region due to the same reason as the depth dose curves.

Two types of layered inhomogeneous phantoms (i.e., water/lung/water and water/bone/water) were used to benchmark the MC calculated central axis depth doses for 4 cm × 4 cm and 10 cm × 10 cm open fields against the measurements. The respective PS_2 files contained 5×10^6 and 3×10^7 particles, and they were recycled 20 times in the phantom simulation. Each phantom consists of 5 cm thick water equivalent phantom (TM water equivalent phantom, Taisei Medical, Osaka, Japan), 10 cm thick lung (lung LN300 model, Gammex-RMI, Middleton, WI, USA) or bone equivalent phantom (Gammex-RMI cortical bone SB3 model), and 10 cm thick water equivalent phantom. In the MC calculation, the x- and y-dimensions of the voxel were set to 0.5 cm. The z-dimension was 0.5 cm in the homogeneous medium and 0.25 cm in the inhomogeneous medium and around the interfaces. The central axis depth doses were measured using the CC-04 ion chamber (Scanditronix Wellhöfer, Schwarzenbruck, Germany) with an active volume of 0.04 cm^3. All the calculated and measured results were normalized to the D_{max} value in a homogeneous phantom for a 10 cm × 10 cm open field. For the measurements, we determined the correction factors, i.e. the products of the restricted collision stopping power ratios $\left((\overline{L}/\rho)^{med}_{gas}\right)$ and the wall correction factor (P_{wall}) for the ion chamber, for both lung and bone media to get the true relative doses.

The results of MCRTV were benchmarked against the EGS4/DOSXYZ results in the ICCR (International Conference on the Use of Computers in Radiation Therapy) accuracy test phantom (Rogers and Mohan 2000), which were taken from the NRCC website (http://www.irs.inms.nrc.ca/papers/iccr00/iccr00.html). The ICCR test phantom consists of the four layers: 3 cm thick water, 2 cm thick aluminium, 7 cm thick lung and 18 cm thick water. The input beam was a uniform 18 MV photon beam from a realistic linear accelerator calculated at NRCC using the EGS4/BEAM code, which were taken from the same website as the phantom. The calculation parameters (including the energy cut-offs for particle transport, the voxel dimensions and the characteristics of the incident photon beam) were fully set in accordance with the ICCR test. The depth dose curves were calculated by MCRTV and the results were compared with those of DOSXYZ.

2.5. Verification of clinical treatment plan calculation

The MC dose calculation for a realistic clinical plan has been performed and the result was compared with that of Eclipse in order to verify the configuration of the beam and patient/phantom in the MCRTV system. We have computed the dose distributions with MC for a prostate IMRT treatment plan created using the Eclipse/Helios system (Varian Medical Systems, Palo Alto, CA, USA) for 15 MV photon beams with five gantry angles (0, 75, 145, 215 and 285°). All the intensity modulated fields were generated using a Mark II 80-leaf MLC. The dose calculation algorithm employed in the Eclipse system was the pencil-beam convolution (PBC) algorithm with modified Batho inhomogeneity corrections. The dose distributions were computed with MCRTV using the treatment plan data transferred from Eclipse and the resulting isodose curves and DVHs for the structures of interest were compared.

3. Results

3.1. Accuracy benchmarks under homogeneous conditions

Figure 3 shows comparisons of ion chamber measured and MC calculated 15 MV photon beam depth dose curves for 6 cm × 6 cm, 10 cm × 10 cm and 20 cm × 20 cm open fields in water. In figure 3(a), the measured values are not corrected for the effective point of measurement, and the MC calculated depth dose curves agreed well with the measurements to within 1% for

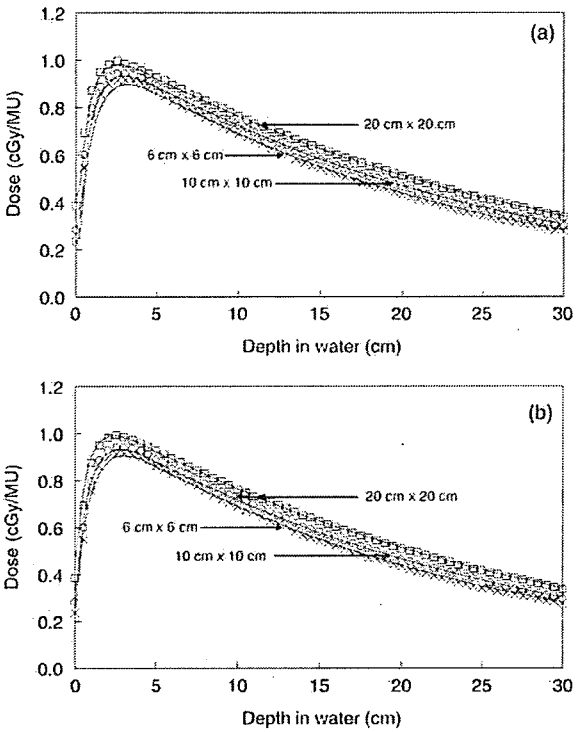

Figure 3. Comparisons of ion chamber measured (lines) and MC calculated (symbols) 15 MV photon beam depth dose curves for 6 cm × 6 cm, 10 cm × 10 cm and 20 cm × 20 cm open fields in water. The measured values are (a) not corrected and (b) corrected for the effective point of measurement. The dose values are expressed in absolute units (cGy MU^{-1}) in order to allow a direct comparison between MC and measurements.

all field sizes, excluding the contaminant electron range. Significant discrepancies were found in the build-up region, where MC consistently predicted higher doses than measurements by up to 10% for a 6 cm × 6 cm field. Figure 3(b) is the same as figure 3(a) but the measured values are corrected for the effective point of measurement. We found the better agreements in the build-up region; however, the discrepancies of about 3% still remained. The agreements at depths beyond the build-up region were maintained within 1%.

Figure 4 shows comparisons of ion chamber measured and MC calculated 15 MV photon beam dose profile curves for 6 cm × 6 cm, 10 cm × 10 cm and 20 cm × 20 cm open fields in water. The agreements between the measured and MC calculated dose profile curves were within 1.5% near the field centre and the differences in the widths of the profiles for given doses were within 1.5 mm for most of the tested field sizes and depths with some exceptions. The MC calculated dose profile curves always gave steeper dose gradients than measurements. The 1σ statistical uncertainties on the MC results were generally less than 1%. As a result of the iterative process to commission the 15 MV photon beam phase-space data, the derived mean energy and the FWHM of intensity distribution of the incident electron beam were 14.5 MeV and 0.17 cm, respectively.

3.2. Accuracy benchmarks under inhomogeneous conditions

Figures 5 and 6 compare the ion chamber measurements and the MC calculated 15 MV photon beam depth dose curves for 4 cm × 4 cm and 10 cm × 10 cm open fields in layered

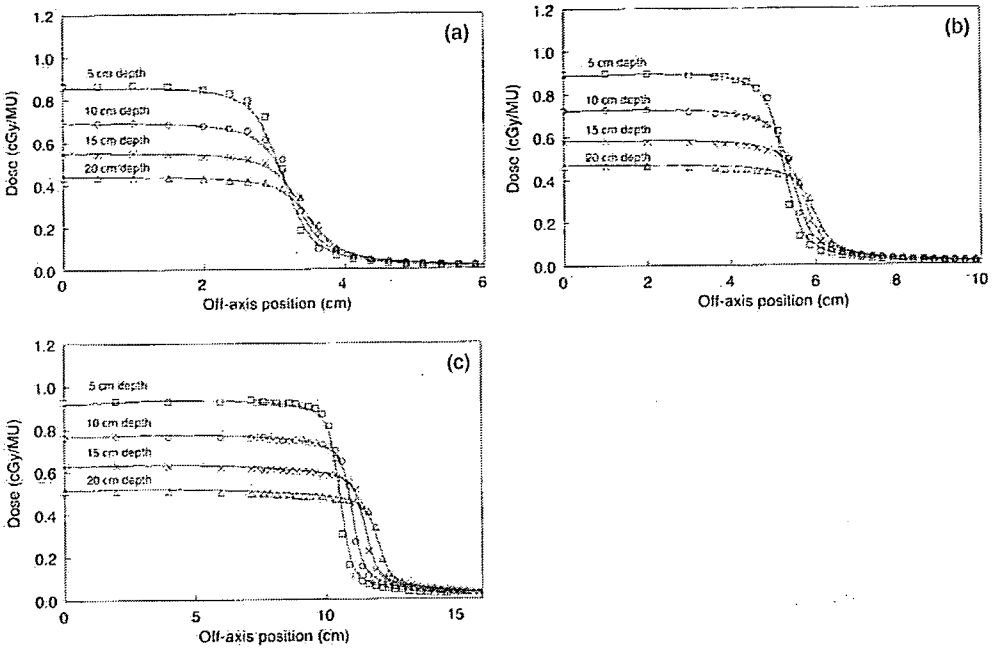

Figure 4. Comparisons of ion chamber measured (lines) and MC calculated (symbols) 15 MV photon beam dose profile curves for (a) 6 cm × 6 cm, (b) 10 cm × 10 cm and (c) 20 cm × 20 cm open fields in water. The dose values are expressed in absolute units (cGy MU^{-1}) in order to allow a direct comparison between MC and measurements.

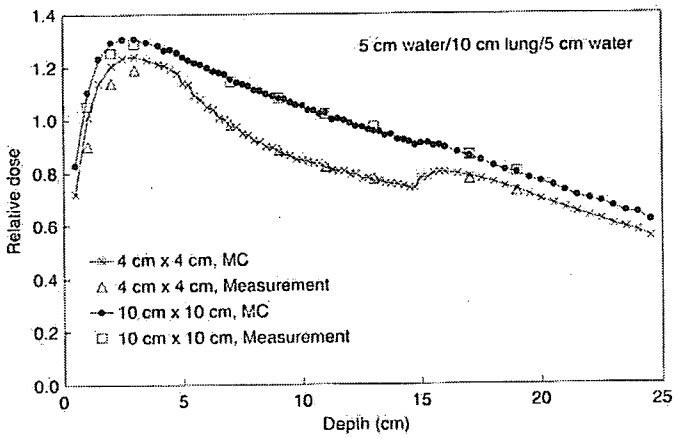

Figure 5. A comparison of ion chamber measured and MC calculated 15 MV photon beam depth dose curves for 4 cm × 4 cm and 10 cm × 10 cm open fields in a layered water/lung/water inhomogeneous phantom. The curves are normalized to the dose at 10 cm depth in a homogeneous phantom for a 10 cm × 10 cm open field.

inhomogeneous phantoms. The curves are normalized to the dose at 10 cm depth in a homogeneous phantom for a 10 cm × 10 cm open field. It was found that the correction factors to obtain the true relative doses for lung and bone media were 0.9809 and 0.8937,

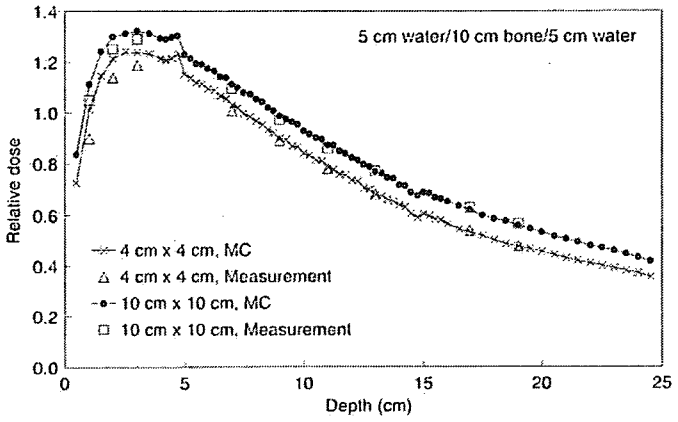

Figure 6. A comparison of ion chamber measured and MC calculated 15 MV photon beam depth dose curves for 4 cm × 4 cm and 10 cm × 10 cm open fields in a layered water/bone/water inhomogeneous phantom. The curves are normalized to the dose at 10 cm depth in a homogeneous phantom for a 10 cm × 10 cm open field.

respectively. Figure 5 shows the depth doses in a water/lung/water inhomogeneous phantom. The depth doses for a 4 cm × 4 cm field showed a severe dose reduction within the lung medium and an increase upon entering the water slab below the inhomogeneity, which was much less discernible for a 10 cm × 10 cm field. Figure 6 shows the depth doses in a water/bone/water inhomogeneous phantom. The depth doses for both of 4 cm × 4 cm and 10 cm × 10 cm fields decreased in the bone slab. At the water/bone interface, the MC calculated depth doses were increased by about 6% and decreased by about 2% at the bone/water interface. Most of the MC calculated depth doses agreed with the measurements to within 1% in both of water/lung/water and water/bone/water phantoms, except in the build-up region, where there were large discrepancies as well as the case of the homogeneous condition (see figure 3). However, relatively large discrepancies of about 2% appeared in the heterogeneous media. The 1σ statistical uncertainties on the MC results were within 1%.

Figure 7 shows a comparison of the 18 MV photon beam depth dose curves for a 1.5 cm × 1.5 cm open field calculated by DOSXYZ and MCRTV in the ICCR test phantom. The curves were normalized to the respective D_{max} values. The MCRTV results showed excellent agreement within 1% with the DOSXYZ results, which were taken from the NRCC website (http://www.irs.inms.nrc.ca/papers/iccr00/iccr00.html). The 1σ statistical uncertainties on the MCRTV results were generally less than 0.5%.

3.3. Verification of clinical treatment plan calculation

Figure 8 shows a comparison of the 15 MV photon beam dose distributions for a prostate IMRT treatment plan calculated by MC and Eclipse. In both calculations, the isodose lines shown represent the relative values normalized to the isocentre dose. The MC calculation required about 15 h CPU time on the entire 28-CPU Linux cluster. It can be seen that the five MC calculated beams generated a dose distribution similar to Eclipse, which indicates that the configuration of the beams and the patient/phantom has been well implemented in MCRTV. There were some dose differences, about 5% between the MC and the Eclipse calculations within or near the bony anatomy. The 1σ statistical uncertainties on the MC results were generally 2%.

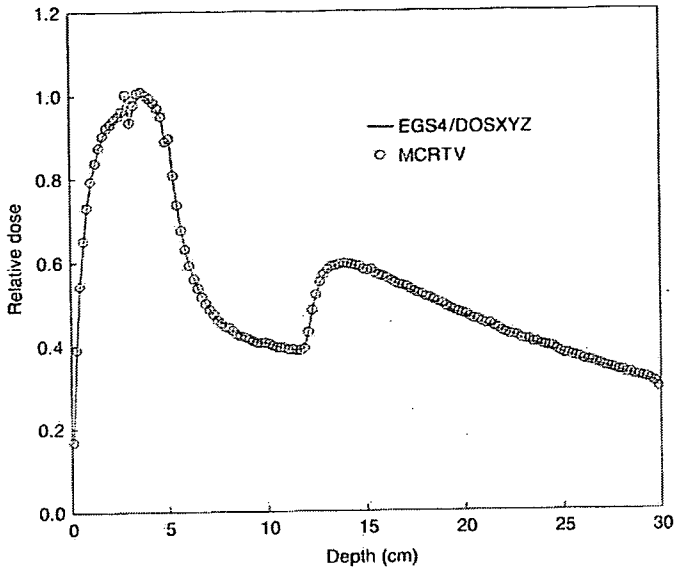

Figure 7. A comparison of the depth dose curves for an 18 MV photon beam calculated by EGS4/DOSXYZ and MCRTV in the ICCR accuracy test phantom (water/aluminium/lung/water). The curves are normalized to the D_{max} value.

4. Discussion

In the commissioning of our clinical 15 MV photon beam phase-space data, the incident electron beam parameters were determined with which MC gives the best match with the measurements. Many investigators have developed the MC models of 6 and 18 MV photon beams from the Varian linear accelerators (Liu *et al* 1997, Fix *et al* 2001b, Hartmann Siantar *et al* 2001, Ding 2002a, Sheikh-Bagheri and Rogers 2002, Chetty *et al* 2003, Keall *et al* 2003, Cho *et al* 2005). There are wide variations among the electron beam shapes (ranging from a pencil beam to cylindrical beams with different sizes) and the derived parameters (mean energy ranging from 5.7 MeV to 6.5 MeV for a 6 MV photon beam), even though all of the studies have reached good agreement between measurements and MC. For a 15 MV photon beam, Chetty *et al* (2003) derived the electron beam energy of 15.3 MeV with a mono-energetic, parallel electron model. Sheikh-Bagheri and Rogers (2002) have derived the mean energy of 14.5 MeV and 0.17 cm FWHM of radial intensity spread using a Gaussian beam model and these values were consistent with our results. Part of the cause of these variations could be attributed to several factors, such as individual differences of the accelerators and methods to model the treatment head components.

Good agreements within 1% between the measured and the MC calculated dose distributions have been obtained in water except the surface. It was found that the correction for the effective point of measurement for the ion chamber had a great impact on the depth dose curve in the build-up region. The correction of the measured depth dose curves gave better agreement with those calculated by MC, though the discrepancies of about 3% still remained. Sheikh-Bagheri and Rogers (2002) and Chetty *et al* (2003) modelled the 15 MV photon beams from their Varian machines and found relatively large differences up to 3% similar to this study. The remaining discrepancies can be attributed to the limitations associated with measurement such as set-up uncertainties and variable stopping power ratios,

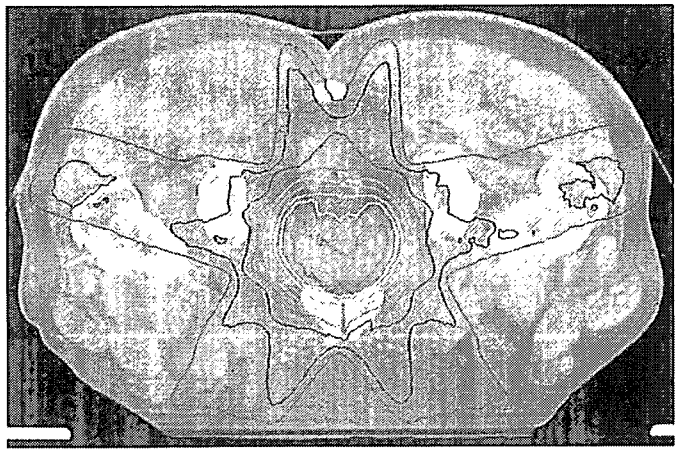

(a)

(b)

Figure 8. A comparison of the 15 MV photon beam dose distributions for a prostate IMRT treatment plan calculated by (a) MC and (b) Eclipse. The isodose lines shown are 30%, 40%, 50%, 60%, 70%, 80%, 90%, 95% and 100% of the isocentre dose.

which have a little impact on the depth dose curves (Sheikh-Bagheri *et al* 2000) and have not been considered in this study. Moreover, it is difficult to accurately convert the ion chamber readings to the doses in the build-up region in part because of the relatively large detector size. Other reasons related to MC, such as the effects of positrons or low-energy photons and the limitations of EGS4 physics models, can also be considered. Several papers have reported a significant discrepancy between MC and measurements in the build-up region in water for 18 MV photon beams (Hartmann Siantar *et al* 2001, Ding 2002a, Keall *et al* 2003). Ding (2002b) and Abdel-Rahman *et al* (2005) have investigated some of the possible causes of such discrepancies (i.e., contaminant charged particles from the accelerator treatment head and triplet production events); however, they could not posit full explanations for them. More thorough studies are required to commission the build-up depth dose curve. Our results of the benchmarks under inhomogeneous conditions were consistent with the findings reported by several authors (DeMarco *et al* 1998, Wang *et al* 1999, Chetty *et al* 2003, Heath *et al* 2004).

Dose perturbations within or near the heterogeneities were well predicted by MC. Relatively large discrepancies that appeared in the heterogeneous regions are probably attributed to the inaccuracy in dose determination under the condition of electronic disequilibrium. More thorough studies on the correction factors are needed to explain such discrepancies.

Relatively large differences between the dose distributions calculated with MCRTV and the commercial TPS shown within or near the bony structures can be explained by inaccuracy of the conventional dose calculation algorithm in the heterogeneities. Dose perturbations at the interface between soft tissue and high- or low-density medium are due to a number of complex effects (Dutreix and Bernard 1966, Bielajew *et al* 1985, Werner *et al* 1987, 1990, Yu *et al* 1995), which lead to the errors in dose computation of the conventional dose algorithms as reported by many investigators (DeMarco *et al* 1998, Ma *et al* 1999, Arnfield *et al* 2000, McDermott *et al* 2003, Carrasco *et al* 2004, Krieger and Sauer 2005). Ma *et al* (1999) compared the heterogeneity correction factors (HCFs) for layered bone and lung phantoms calculated by MC, fast Fourier transform (FFT) convolution, and superposition convolution algorithms in a commercial TPS (FOCUS, CMS, St Louis, MO, USA). They found uncertainties in the calculated HCFs of up to 10% for the FFT convolution algorithm. With the superposition convolution algorithm, more accurate results were obtained; however, there were still large uncertainties near the interfaces. Such perturbations can be accounted for by the MC simulation and this is expected as a powerful methodology to detect the regions where the conventional dose algorithms fail to predict the accurate dose distributions, i.e., MC treatment plan verification.

There have been several MC dose calculation systems, such as MCDOSE of Stanford University and Fox Chase Cancer Center (Ma *et al* 2002), RT_DPM of University of Michigan (Chetty *et al* 2003) and MCV of Virginia Commonwealth University (Siebers *et al* 2000), which are used for full MC treatment planning or treatment plan verification. They employ a variety of variance reduction and efficiency improving techniques to speed up the MC computation time. Whereas we have employed only one variance reduction technique (i.e. bremsstrahlung splitting) for the patient-independent portion of the treatment head, since MCRTV was originally designed to provide the dose calculation benchmark results as accurately as possible, even though a relatively long CPU time is needed. MCRTV is much less efficient and slower than the fast MC codes, as mentioned above; however, the overall CPU time for the calculation of a realistic treatment plan is acceptable for the clinical use of MCRTV as a routine IMRT QA tool in our clinics. The MCRTV system now implements only one well-commissioned set of phase-space data for the 15 MV photon beam from our Varian Clinac 2300C/D accelerator. The photon beams with other nominal energies of 4 and 6 MV from a Varian Clinac 2300C/D and a 600EX, respectively, will also be modelled to deal with more treatment modalities and sites. Moreover, future work will concentrate on modelling the Varian Millennium 120-leaf MLC to be introduced to our clinics, and detailed verification of the MLC models, including the Mark II developed in the present study. We are willing to make the MCRTV system available to the public in the future.

5. Conclusions

An integrated MC dose calculation system, MCRTV, has been developed for clinical treatment plan verification, especially for routine IMRT plan QA. We have presented the key features of the MCRTV system and demonstrated the feasibility of its clinical application. The phase-space data of our 15 MV photon beam have been developed, and several benchmarks have been performed under homogeneous and several inhomogeneous conditions, including high- and low-density media. The MC results showed good agreement with the measurements

to within 1% and 2% for homogeneous and inhomogeneous conditions, respectively. An MCRTV calculation for a prostate IMRT treatment plan validated the implementation of the beams and the patient/phantom configuration.

Acknowledgments

This study was supported in part by a Grant-in-Aid for Scientific Research from the Japanese Ministry of Health, Labor and Welfare (No. H16-039, 'Third-Term Comprehensive Control Research for Cancer'), a Grant-in-Aid for Scientific Research from the Japan Society for the Promotion of Science (No. 16390338), a Grant-in-Aid for Scientific Research on Priority Areas Cancer from the Japanese Ministry of Education, Culture, Sports, Science and Technology (No. 17016036), and a Grant-in-Aid for Scientific Research from the Japanese Ministry of Education, Culture, Sports, Science and Technology (No. 17390333). The authors would like to thank Calvin Huntzinger, Stanley Johnsen, Chudo Kazusa and Hiroyuki Kawaguchi of Varian Medical Systems for providing detailed information of the Clinac 2300C/D and the Mark II MLC used for the MC simulation in our study. We would like to express our appreciation to Dr Jeffrey Siebers and Dr Paul Keall of Virginia Commonwealth University for fruitful discussion and information on MC modelling of a Varian 15 MV photon beam. We are also grateful to Dr Hideo Hirayama and Dr Yoshihito Namito of the High Energy Accelerator Research Organization (KEK) for their technical advice regarding the EGS4 Monte Carlo simulation.

References

AAPM TG-65 2004 Tissue inhomogeneity corrections for megavoltage photon beams *AAPM Report No.* 85 (Madison, WI: Medical Physics Publishing) p 9

Abdel-Rahman W, Seuntjens J P, Verhaegen F, Deblois F and Podgorsak E B 2005 Validation of Monte Carlo calculated surface doses for megavoltage photon beams *Med. Phys.* **32** 286–98

Arnfield M R, Hartmann Siantar C, Siebers J V, Garmon P, Cox L and Mohan R 2000 The impact of electron transport on the accuracy of computed dose *Med. Phys.* **27** 1266–74

Bieda M R, Antolak J A and Hogstrom K R 2001 The effect of scattering foil parameters on electron-beam Monte Carlo calculations *Med. Phys.* **28** 2527–34

Bielajew A F, Mohan R and Chui C-S 1989 Improved bremsstrahlung photon angular sampling in the EGS4 code system *National Research Council of Canada Report* PIRS-0203 (Ottawa: NRCC)

Bielajew A F and Rogers D W O 1987 PRESTA: the parameter reduced electron-step transport algorithm for electron Monte Carlo transport *Nucl. Instrum. Methods* B **18** 165–81

Bielajew A F, Rogers D W O and Nahum A E 1985 The Monte Carlo simulation of ion chamber response to ^{60}Co-resolution of anomalies with interfaces *Phys. Med. Biol.* **30** 419–27

Brooks R A, Mitchell L G, O'Connor C M and Di Chiro G 1981 On the relationship between computed tomography numbers and specific gravity *Phys. Med. Biol.* **26** 141–7

Carrasco P, Jornet N, Duch M A, Weber L, Ginjaume M, Eudaldo T, Jurado D, Ruiz A and Ribas M 2004 Comparison of dose calculation algorithms in phantoms with lung equivalent heterogeneities under conditions of lateral electronic disequilibrium *Med. Phys.* **31** 2899–911

Chetty I J, Charland P M, Tyagi N, McShan D L, Fraass B A and Bielajew A F 2003 Photon beam relative dose validation of the DPM Monte Carlo code in lung-equivalent media *Med. Phys.* **30** 563–73

Cho S H, Vassiliev O N, Lee S, Liu H H, Ibbott G S and Mohan R 2005 Reference photon dosimetry data and reference phase space data for the 6 MV photon beam from Varian Clinac 2100 series linear accelerators *Med. Phys.* **32** 137–48

Cygler J E, Daskalov G M, Chan G H and Ding G X 2004 Evaluation of the first commercial Monte Carlo dose calculation engine for electron beam treatment planning *Med. Phys.* **31** 142–53

DeMarco J J, Solberg T D and Smathers J B 1998 A CT-based Monte Carlo simulation tool for dosimetry planning and analysis *Med. Phys.* **25** 1–11

Ding G X 2002a Energy spectra, angular spread, fluence profiles and dose distributions of 6 and 18 MV photon beams: results of Monte Carlo simulations for a Varian 2100EX accelerator *Phys. Med. Biol.* **47** 1025–46

Ding G X 2002b Dose discrepancies between Monte Carlo calculations and measurements in the buildup region for a high-energy photon beam *Med. Phys* **29** 2459–63

Dutreix J and Bernard M 1966 Dosimetry at interfaces for high energy X and gamma rays *Br. J. Radiol.* **39** 205–10

Fippel M 1999 Fast Monte Carlo dose calculation for photon beams based on the VMC electron algorithm *Med. Phys.* **26** 1466–75

Fippel M, Kawrakow I and Friedrich K 1997 Electron beam dose calculations with the VMC algorithm and the verification data set of the NCI working group *Phys. Med. Biol.* **42** 501–20

Fix M K, Manser P, Born E J, Mini R and Rüegsegger P 2001a Monte Carlo simulation of a dynamic MLC based on a multiple source model *Phys. Med. Biol.* **46** 3241–57

Fix M K, Stampanoni M, Manser P, Born E J, Mini R and Rüegsegger P 2001b A multiple source model for 6 MV photon beam dose calculations using Monte Carlo *Phys. Med. Biol.* **46** 1407–27

Francescon P, Cora S and Chiovati P 2003 Dose verification of an IMRT treatment planning system with the BEAM EGS4-based Monte Carlo code *Med. Phys.* **30** 144–57

Hartmann Siantar C L *et al* 2001 Description and dosimetric verification of the PEREGRINE Monte Carlo dose calculation system for photon beams incident on a water phantom *Med. Phys.* **28** 1322–37

Heath E *et al* 2004 Dosimetric evaluation of the clinical implementation of the first commercial IM R T Monte Carlo treatment planning system at 6 MV *Med. Phys.* **31** 2771–9

ICRU 1976 Determination of absorbed dose in a patient by beams of X or gamma rays in radiotherapy procedures *ICRU Report* 24 (Bethesda, MD: ICRU)

ICRU 1987 Use of computers in external beam radiotherapy procedures with high-energy photons and electrons *ICRU Report* 42 (Bethesda, MD: ICRU)

ICRU 1989 Tissue substitutes in radiation dosimetry and measurement *ICRU Report* 44 (Bethesda, MD: ICRU)

Johnsen S and Siebers J V 2005 Personal communication

Kawrakow I 2001 VMC++, electron and photon Monte Carlo calculations optimized for radiation treatment planning *Advanced Monte Carlo for Radiation Physics, Particle Transport Simulation and Applications: Proc. Monte Carlo 2000 Meeting (Lisbon, Portugal)* ed A Kling *et al* (Berlin: Springer) pp 229–36

Kawrakow I and Fippel M 2000 Investigation of variance reduction techniques for Monte Carlo photon dose calculation using XVMC *Phys. Med. Biol.* **45** 2163–84

Kawrakow I, Fippel M and Friedrich K 1996 3D electron dose calculation using a voxel Monte Carlo algorithm (VMC) *Med. Phys.* **23** 445–57

Kawrakow I and Rogers D W O 2003 The E G Snrc code system: Monte Carlo simulation of electron and photon transport *National Research Council of Canada Report* PIRS-701 (Ottawa: NRCC)

Keall P J, Siebers J V, Libby B and Mohan R 2003 Determining the incident electron fluence for Monte Carlo-based photon treatment planning using a standard measured data set *Med. Phys.* **30** 574–82

Kim J O, Siebers J V, Keall P J, Arnfield M R and Mohan R 2001 A Monte Carlo study of radiation transport through multileaf collimators *Med. Phys.* **28** 2497–506

Krieger T and Sauer O A 2005 Monte Carlo-versus pencil-beam-/collapsed-cone-dose calculation in a heterogeneous multi-layer phantom *Phys. Med. Biol.* **50** 859–68

Liu H H, Mackie T R and McCullough E C 1997 A dual source photon beam model used in convolution/superposition dose calculations for clinical megavoltage x-ray beams *Med. Phys.* **24** 1960–74

Liu H H, Mackie T R and McCullough E C 2000 Modeling photon output caused by backscattered radiation into the monitor chamber from collimator jaws using a Monte Carlo technique *Med. Phys.* **27** 737–44

Liu H H, Verhaegen F and Dong L 2001 A method of simulating dynamic multileaf collimators using Monte Carlo techniques for intensity-modulated radiation therapy *Phys. Med. Biol.* **46** 2283–98

LoSasso T, Chui C-S and Ling C C 1998 Physical and dosimetric aspects of a multileaf collimation system used in the dynamic mode for implementing intensity modulated radiotherapy *Med. Phys.* **25** 1919–27

Lovelock D M J, Chui C-S and Mohan R 1995 A Monte Carlo model of photon beams used in radiation therapy *Med. Phys.* **22** 1387–94

Ma C-M, Li J S, Pawlicki T, Jiang S B, Deng J, Lee M C, Koumrian T, Luxton M and Brain S 2002 A Monte Carlo dose calculation tool for radiotherapy treatment planning *Phys. Med. Biol.* **47** 1671–89

Ma C-M, Mok E, Kapur A, Pawlicki T, Findley D, Brain S, Forster K and Boyer A L 1999 Clinical implementation of a Monte Carlo treatment planning system *Med. Phys.* **26** 2133–43

Ma C-M, Pawlicki T, Jiang S B, Li J S, Deng J, Mok E, Kapur A, Xing L, Ma L and Boyer A L 2000 Monte Carlo verification of IMRT dose distributions from a commercial treatment planning optimization system *Phys. Med. Biol.* **45** 2483–95

Ma C-M, Reckwerdt P J, Holmes M, Rogers D W O and Geiser B 1995 DOSXYZ Users Manual *National Research Council of Canada Report* PIRS-509B (Ottawa: NRCC)

Mackie T R 1990 Applications of the Monte Carlo method in radiotherapy *The Dosimetry of Ionizing Radiation* vol 3 ed K Kase *et al* (New York: Academic) pp 541–620

McDermott P N, He T and DeYoung A 2003 Dose calculation accuracy of lung planning with a commercial IMRT treatment planning system *J. Appl. Clin. Med. Biol.* **4** 341–51

Mohan R 1997 Why Monte Carlo? *Proc. 12th Int. Conf. on the Use of Computers in Radiation Therapy (ICCR) (Salt Lake City, UT, USA)* ed D D Leavitt and G Starkschall (Madison, WI: Medical Physics Publishing) pp 16–8

Nelson W R, Hirayama H and Rogers D W O 1985 The EGS4 code system *Stanford Linear Accelerator Center Report* SLAC-265 (Stanford, CA: SLAC)

Rogers D W O and Mohan R 2000 Questions for comparison of clinical Monte Carlo code *Proc. 13th Int. Conf. on the Use of Computers in Radiation Therapy (ICCR) (Heidelberg, Germany)* ed W Schlegel and T Bortfeld (Berlin: Springer) pp 120–2

Sakthi N, Keall P J, Mihaylov I, Wu Q, Wu Y, Williamson J F, Schmidt-Ullrich R and Siebers J V 2006 Monte Carlo-based dosimetry of head-and-neck patients treated with SIB-IMRT *Int. J. Radiat. Oncol. Biol. Phys.* **64** 968–77

Sempau J, Wilderman S J and Bielajew A F 2000 DPM, a fast, accurate Monte Carlo code optimized for photon and electron radiotherapy treatment planning dose calculations *Phys. Med. Biol.* **45** 2263–91

Sheikh-Bagheri D and Rogers D W O 2002 Sensitivity of megavoltage photon beam Monte Carlo simulations to electron beam and other parameters *Med. Phys.* **29** 379–90

Sheikh-Bagheri D, Rogers D W O, Ross C K and Seuntjens J P 2000 Comparison of measured and Monte Carlo calculated dose distributions from the NRC linac *Med. Phys.* **27** 2256–66

Siebers J V and Keall P J 2005 Personal communication

Siebers J V, Keall P J and Kawrakow I 2005 Monte Carlo dose calculations for external beam radiation therapy *The Modern Technology of Radiation Oncology* vol 2 ed J Van Dyk (Madison, WI: Medical Physics Publishing) p 94

Siebers J V, Keall P J, Kim J O and Mohan R 2000 Performance benchmarks of the MCV Monte Carlo system *Proc. 13th Int. Conf. on the Use of Computers in Radiation Therapy (ICCR) (Heidelberg, Germany)* ed W Schlegel and T Bortfeld (Berlin: Springer) pp 129–31

Siebers J V, Keall P J, Libby B and Mohan R 1999 Comparison of EGS4 and MCNP4b Monte Carlo codes for generation of photon phase space distributions for a Varian 2100C *Phys. Med. Biol.* **44** 3009–26

Tyagi N, Bose A and Chetty I J 2004 Implementation of the DPM Monte Carlo code on a parallel architecture for treatment planning applications *Med. Phys.* **31** 2721–5

Verhaegen F and Seuntjens J 2003 Monte Carlo modelling of external radiotherapy photon beams *Phys. Med. Biol.* **48** R107–64

van Santvoort J P and Heijmen B J 1996 Dynamic multileaf collimation without 'tongue-and-groove' underdosage effects *Phys. Med. Biol.* **41** 2091–105

Walters B R B, Kawrakow I and Rogers D W O 2002 History by history statistical estimators in the BEAM code system *Med. Phys.* **29** 2745–52

Wang L, Lovelock M and Chui C-S 1999 Experimental verification of a CT-based Monte Carlo dose-calculation method in heterogeneous phantoms *Med. Phys.* **26** 2626–34

Wang L, York E and Chui C-S 2002 Monte Carlo evaluation of 6 MV intensity modulated radiotherapy plans for head and neck and lung treatments *Med. Phys.* **29** 2705–17

Webb S, Bortfeld T, Stein J and Convery D 1997 The effect of stair-step leaf transmission on the 'tongue-and-groove problem' in dynamic radiotherapy with a multileaf collimator *Phys. Med. Biol.* **42** 595–602

Werner B L, Das I J, Khan F M and Meigooni A S 1987 Dose perturbations at interfaces in photon beams *Med. Phys.* **14** 585–95

Werner B L, Das I J and Salk W N 1990 Dose perturbations at interfaces in photon beams: secondary electron transport *Med. Phys.* **17** 212–26

Yang J, Li J, Chen L, Price R, McNeeley S, Qin L, Wang L, Xiong W and Ma C-M 2005 Dosimetric verification of IMRT treatment planning using Monte Carlo simulations for prostate cancer *Phys. Med. Biol.* **50** 869–78

Yu C X, Mackie T R and Wong J W 1995 Photon dose calculation incorporating explicit electron transport *Med. Phys.* **22** 1157–65

ELSEVIER MASSON

Disponible en ligne sur www.sciencedirect.com

ScienceDirect

Cancer/Radiothérapie 11 (2007) 32–35

CANCER RADIOTHÉRAPIE

http://france.elsevier.com/direct/CANRAD/

Review

Stereotactic body radiation therapy (SBRT) for early-stage lung cancer

Radiothérapie stéréotaxique pour cancer bronchique localisé

M. Hiraoka*, Y. Matsuo, Y. Nagata

Department of Radiation Oncology and Image-applied Therapy, Kyoto University Graduate School of Medicine, Sakyo, Kyoto, Japan

Available online 08 December 2006

Abstract

Stereotactic body radiation therapy (SBRT) is a new treatment modality for early-stage non-small-cell lung cancer, and has been developed in the United States, the European Union, and Japan. We started a feasibility study of this therapy in July 1998, using a stereotactic body frame. The eligibility criteria for primary lung cancer were: 1) solitary tumor less than 4 cm (T1-3N0M); 2) inoperable, or the patient refused operation; 3) no necessity for oxygen support; 4) performance status equal to or less than 2; 5) the peripheral tumor which dose constraints of mediastinal organs are maintained. A total dose of 48 Gy was delivered in four fractions in 2 weeks in most patients. Lung toxicity was minimal. No grade II toxicities for spinal cord, bronchus, pulmonary artery, or esophagus were observed. The 3 years overall survival for 32 patients with stage IA, and 13 patients with stage IB were 83% and 72%, respectively. Only one local recurrence was observed in a follow-up of 6–71 months. We retrospectively analyzed 241 patients from 13 Japanese institutions. The local recurrence rate was 20% when the biological equivalent dose (BED) was less than 100 Gy, and 6.5% when the BED was over 100 Gy. Overall survival at 3 years was 42% when the BED was less than 100 Gy, and 46% when it was over 100 Gy. In tumors, which received a BED of more than 100 Gy, overall survival at 3 years was 91% for operable patients, and 50% for inoperable patients. Long-term results, in terms of local control, regional recurrence, survival, and complications, are not yet evaluated. However, this treatment modality is highly expected to be a standard treatment for inoperable patients, and it may be an alternative to lobectomy for operative patients. A prospective trial, which is now ongoing, will, answer these questions.

Résumé

La radiothérapie stéréotaxique extracérébrale est une nouvelle modalité thérapeutique du carcinome bronchique non à petites cellules localisé. Cette technique a été développée aux États-Unis, en Europe et au Japon. Nous avons débuté en juillet 1998 une étude de faisabilité de ce traitement avec l'aide d'un cadre stéréotactique corporel. Les critères d'éligibilité pour le cancer bronchique primitif étaient : 1) tumeur isolée de moins de 4 cm (T1-3N0M0) ; 2) tumeur non résécable ou patient refusant la chirurgie ; 3) pas de nécessité d'avoir recours à une oxygénothérapie ; 4) indice de performance égal ou inférieur à 2 ; 5) tumeur périphérique n'entraînant pas une irradiation à dose très importante du médiastin. Une dose totale de 48 Gy a été délivrée en quatre fractions et deux semaines. Chez la plupart des patients, la toxicité pulmonaire a été minimale. Aucune toxicité de grade II n'a été observée pour la moelle épinière, les bronches, les artères pulmonaires ou l'œsophage. Les taux de survie globale à trois ans des 32 patients atteints d'un cancer de stade IA et 13 de stade IB étaient respectivement de 83 et 72 %. Une seule récidive locale a été observée pendant une période de suivi de 6 à 71 mois. Nous avons par ailleurs, rétrospectivement, analysé les résultats obtenus dans une série de 241 patients traités dans 13 institutions japonaises. Le taux de récidive local était de 20 % quand la dose biologique équivalente (BED) était inférieure à 100 Gy, et de 6,5 % quand elle était supérieure à 100 Gy. Le taux de survie à trois ans était de 42 % quand la BED était inférieure à 100 Gy et 46 % quand elle était supérieure. Lorsque la BED était supérieure à 100 Gy, le taux de survie à trois ans était de 91 %, pour les patients atteints d'une tumeur résécable, et 50 % pour les patients inopérables. Les résultats à long terme, en termes de contrôle local, récidive locale, survie et complications ne sont pas encore évalués. Cependant, cette modalité thérapeutique est d'ores et déjà considérée comme le traitement standard pour les patients inopérables et sera une possible alternative à une lobectomie pour les patients opérables. Un essai prospectif en cours permettra de répondre à ces questions.

Keywords: Non-small-cell lung cancer; Stereotactic body radiation therapy

Mots clés : Cancer bronchique non à petites cellules ; Irradiation stéréotactique extracrânienne

* Corresponding author.

1278-3218/$ - see front matter © 2006 Elsevier Masson SAS. All rights reserved.
doi:10.1016/j.canrad.2006.11.001

Stereotactic body radiation therapy (SBRT) for early-stage non-small-cell lung cancer (NSCLC) is a new treatment modality, and Japan is one of the leading countries in this three-dimensional radiation therapy. The background of this treatment is the great success of stereotactic irradiation for intracranial tumors, in terms of the technologies used, quality assurance (QA) and quality control (QC), and clinical outcomes. That is, a high local control rate has been shown with minimal toxicities. The success has caused much interest in the application of this treatment for extracranial regions [1,5,13]. Why use stereotactic radiation irradiation (SRI) for lung cancer? The number of patients detected at an early-stage has been increased by screening examinations. Accordingly, the number of older patients with early-stage lung cancer who are not amenable to operation has increased, and the clinical results of conventional radiation therapy are not satisfactory. In regard to technical aspects, the application of this new technique is easier for lung cancer, because it is visible on fluoroscopy and because normal tissue toxicities to radiation are relatively well described compared with other normal tissues.

For the management of stage I NSCLC, surgical resection alone is the standard treatment, and lobectomy is generally accepted as the optimal surgical procedure. Survival outcomes of surgical treatment has recently been reported by the Japanese Association for Chest Surgery. According to these data, the overall survival of patients in clinical stage IA is 81.3% at 3 years, and 71.5% at 5 years, and that of patients in clinical stage IB is 62.9% at 3 years, and 50.1% at 5 years.

What about radiation therapy alone for stage I NSCLC? As is known, radiation therapy has been used primarily for those patients who are not considered to be surgical candidates; that is, those who refuse surgical intervention, and those who are medically inoperable. The reported 5 years survival rate is around 8–27%, and is not satisfactory. Several prognostic factors, such as T stage and total dose, have been reported, and doses higher than 65 Gy did show higher survival rates, which can be a rationale for dose escalation (Table 1).

However, there remain several problems with stereotactic radiation therapy for lung cancer compared to its use in intracranial tumors:

- How should the body be fixed with high accuracy?
- How do we cope with the movement of the tumor caused by respiration?
- What are the optimal treatment regimens?
- Toxicities to normal tissue caused by large-fraction size irradiation have not been examined.
- Fractionated stereotactic radiation therapy is considered to be appropriate for lung cancer, but the optimal fractionation scheme has not yet been decided.

We started a feasibility study of this SBRT for small lung tumors in July 1998 [7,8]. The treatment planning with multiple non-coplanar beams is shown in Fig. 1. The patient was placed in this body frame, and immobilized. We used both X-ray and computed tomography (CT) simulators, with the same table, to improve the accuracy of the setup. The movement of the tumor caused by respiration was estimated using fluoroscopy, and if that movement in the craniocaudal (CC) direction was greater than 8 mm, a diaphragm control was employed to suppress the movement of the chest wall. Then the three-dimensional treatment planning was carried out. We verified the tumor location in each treatment. As regards the movement of the tumor caused by respiration, the largest movement was in the CC direction. It was 0–22 mm, and

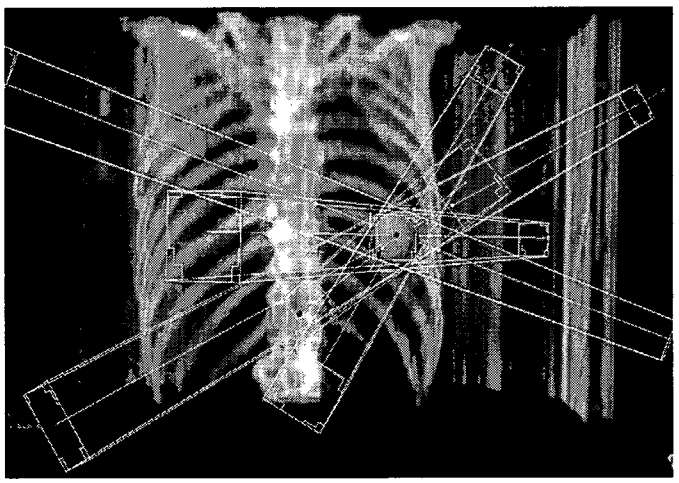

Fig. 1. SBRT for stage I lung cancer.

Table 1
Summary of the results on SBRT for primary lung cancer

Author (Refs.)	Year	Number of patients	Median follow-up (months)	Prescribed dose	Reference point	Isocenter dose (Gy)	BED[a] (Gy)	Overall survival rate (%)	Local control rate (%)
Uematsu et al. [14]	2001	50	36	50–60 Gy/5–10 fr.	Isocenter	50–60	96–100	66 (3 years)	94
Fukumoto et al. [3]	2002	22	24	48–60 Gy/8 fr.	Isocenter	48–60	76.8–105	NA	94
Hof et al. [4]	2003	10	15	19–26 Gy/1 fr.	Isocenter	19–26	55.1–93.6	64	80
Wulf et al. [15]	2004	20	11	30–37.5 Gy/3 fr.	Periphery	45–56.25	113–162	32	92
Onishi et al. [11]	2004	35	13	60 Gy/10 fr.	Periphery	70–75	119–131	58	94
McGarry et al. [6]	2005	47	27 (T1), 19 (T2)	24–72 Gy/3 fr.	Periphery	30–90	60–360	NA	79
Zimmermann et al. [17]	2005	30	18	37.5 Gy/3 fr.	Periphery	62.5	193	75	87
Nagata et al. [7]	2005	45	30	48 Gy/4 fr.	Isocenter	48	106	83 (T1), 72 (T2)	98
Nyman et al. [9]	2006	45	43	45 Gy/3 fr.	Periphery	63	195	71	80
Beitler et al. [2]	2006	75	17	40 Gy/5 fr.	Periphery	47	91.2	45	NA

[a] Biologically effective dose at the isocenter with α/β ratio of 10.

movement of less than 15 mm occurred in 90% of all tumors. When that movement was over 20 mm, we used the diaphragm control, and, with the use of this device, the movement of the respiration decreased significantly. The set-up error with patients was greater than 3 min in at least one direction. Patient repositioning had to be undertaken in 21.6% of all treatments.

The eligibility criteria for primary lung cancer were as follows: solitary tumor less than 4 cm; inoperable, or the patient refused operation; histologically confirmed malignancy; no necessity for oxygen support; performance status equal to or less than 2; and the tumor was not close to spinal cord.

The eligibility criteria for metastatic lung cancer were as follows: one to two tumors less than 4 cm each, primary tumor controlled, no other metastasis, no necessity for oxygen support, performance status less than 2, and tumors not close to the spinal cord. Between July 1998 and November 2005, a total of 147 patients received this treatment modality. Their ages ranged from 17 to 87 years, with a mean of 74 years. Seventy-nine patients had primary tumors, and 54 patients had secondary tumors. In 115 tumors, a total dose of 48 Gy was delivered, in four fractions in 2 weeks. Twenty-seven tumors were treated with a total dose of up to 60 Gy in five fractions. In the initial three tumors, a total dose of 40 Gy was administered.

Survival curves for 32 patients with stage IA, TINOMO NSCLC are shown in Fig. 2. One local recurrence was observed in a follow-up of 6–71 months (median, 30 months). Intrapulmonary recurrence developed in four patients, regional lymph node recurrence developed in two patients, and bone metastases developed in one patient.

Survival curves for 13 patients with stage IB, T2NOMO NSCLC are shown in Fig. 3. No local recurrence was observed at a follow-up of 6–64 months (median, 22 months). Intrapulmonary recurrence developed in four patients, liver and brain metastases developed in one patient each.

We examined the toxicity by National Cancer Institute Common Toxicity Criteria (NCI-CTC) version 2. Lung toxicity was grade II in 4% and grade I in 96%. No grade II toxicities for spinal cord, bronchus, pulmonary artery, or esophagus were observed. The clinical course of one patient who responded well to this treatment is shown in Fig. 4.

We retrospectively analyzed data from 241 patients from 13 Japanese institutes [10]. Their ages ranged from 35 to 92 years, with a median of 76 years. Histology was squamous cell carcinoma in 106 patients, adenocarcinoma in 102 patients, and "others" in 33 patients. As regards clinical stage, 153 patients were stage IA, and 88 patients were stage IB. Tumor diameter ranged from 7 to 58 mm, with a median of 28 mm. One hundred and sixty-one patients were inoperable, and 80 patients were operable. The biological equivalent dose (BED) was 57–180 Gy, with a median of 108 Gy.

Lung toxicities were minimal, with grade II in only 2.2% and no grade III. Local response to the treatment was complete response (CR) in 23%, and partial response (PR) in 62%. The local recurrence rate was 20% when BED was less than 100 Gy, and 6.5% when BED was over 100 Gy, at follow-up periods of 4–72 months (median, 18 months). Overall survival at 3 years was 42% when BED was less than 100 Gy, and 46% when BED was over 100 Gy. For tumors, which received a BED of more than 100 Gy, overall survival at 3 years was 91% for operable patients, and 50% for inoperable patients.

Based upon several good clinical results [2,3,6,12,14–17], we have started a prospective multiinstitutional phase II study with a grant from the Health and Welfare Ministry of Japan. The target is stage IA NSCLC. A total dose of 48 Gy in four fractions will be delivered in 4–8 days. Entry of 165 patients from 16 institutes in 3 years is expected. By the end of May 2006, 85 patients were entried. The primary endpoint is survival. This is the first trial of the Radiation Therapy Study Group (RTSG), which is the newest group in the Japanese Clinical Oncology Group (JCOG). We hope that this trial will provide more conclusive data on stereotactic body irradiation for early-stage NSCLC.

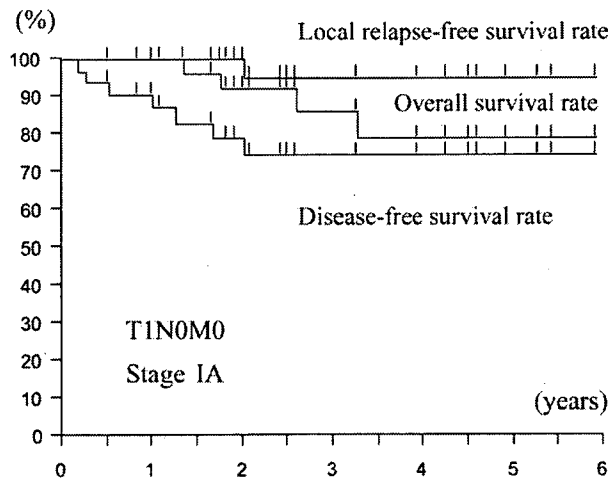

Fig. 2. Survival curves of patients with stage IA: T1N0M0 NSCLC treated with SBRT.

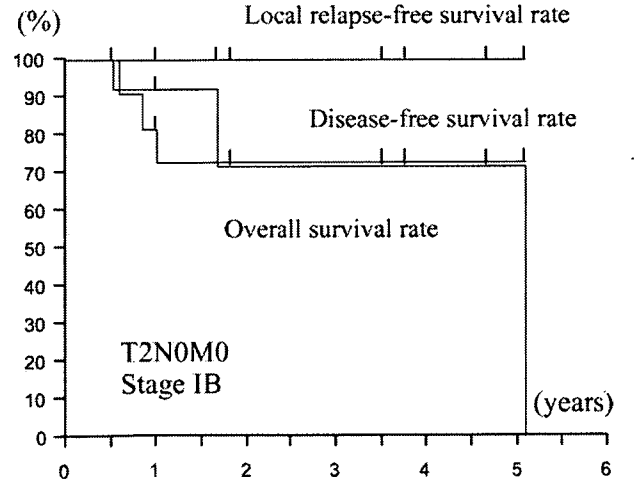

Fig. 3. Survival curves of patients with stage IB: T2N0M0 NSCLC treated with SBRT.

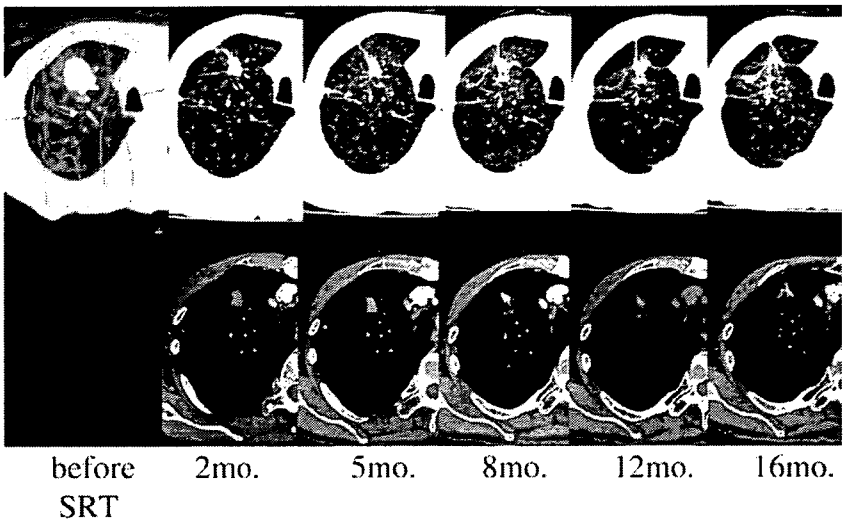

Fig. 4. Clinical course of a patient treated with SBRT. The patient, a 71-year-old man, had primary lung cancer (squamous cell carcinoma; T2N0M0).

In summary, regarding SBRT for early-stage NSCLC:

- long-term results, in terms of local control, regional recurrence, survival, and complications are not yet evaluated;
- technologies to cope with tumor movement, gauging tracking, need to be improved;
- this treatment modality is highly expected to be a standard treatment for inoperable patients, and may be an alternative to lobectomy for operative patients.

A prospective trial ongoing is expected to resolve these matters.

References

[1] Blomgren H, Lax I, Goeranson H, Kraepelien T, Nilsson B, Naslund I, et al. Radiosurgery for tumors in the body: clinical experience using a new method. J Radiosurg 1998;1:63–74.

[2] Beitler JJ, Badine EA, El-Sayah D, Makara D, Friscia P, Silverman P, et al. Stereotactic body radiation therapy for nonmetastatic lung cancer: an analysis of 75 patients treated over 5 years. Int J Radiat Oncol Biol Phys 2006;65:100–6.

[3] Fukumoto S, Shirato H, Shimzu S, Ogura S, Onimaru R, Kitamura K, et al. Small-volume image-guided radiotherapy using hypofractionated, coplanar, and noncoplanar multiple fields for patients with inoperable stage I nonsmall cell lung carcinomas. Cancer 2002;95:1546–53.

[4] Hof H, Herfarth KK, Munter M, Hoess A, Motsch J, Wannenmacher M, et al. Stereotactic single-dose radiotherapy of stage I non-small-cell lung cancer (NSCLC). Int J Radiat Oncol Biol Phys 2003;56:335–41.

[5] Lax I, Blomgren H, Larson D, Naslund I. Extracranial stereotactic radiosurgery of localized target. J Radiosurg 1998;1:135–48.

[6] McGarry RC, Papiez L, Williams M, Whiteford T, Timmerman RD. Stereotactic body radiation therapy of early-stage non-small cell lung carcinoma: Phase I study. Int J Radiat Oncol Biol Phys 2005;63:1010–5.

[7] Nagata Y, Takayama K, Matsuo Y, Norihisa Y, Mizowaki T, Sakamoto T, et al. Clinical outcomes of a Phase I/II study of 48 Gy of stereotactic body radiation therapy in 4 fractions for primary lung cancer using a stereotactic body frame. Int J Radiat Oncol Biol Phys 2005;63(5):1427–31.

[8] Negoro Y, Nagata Y, Aoki T, Mizowaki T, Takayama K, Kokubo M, et al. The effectiveness of an immobilization device in conformal radiotherapy for lung tumor: reduction of respiratory tumor movement and evaluation of daily set-up accuracy. Int J Radiat Oncol Biol Phys 2001; 50:889–98.

[9] Nyman J, Johansson KA, Hulten U. Stereotactic hypofractionated radiotherapy for stage I non-small cell lung cancer—mature results for medically inoperable patients. Lung Cancer 2006;51:97–103.

[10] Onishi H, Araki T, Shirato H, Nagata Y, Hiraoka M, Gomi K, et al. Stereotactic hypofractionated high-dose irradiation for stage I nonsmall cell lung carcinoma. Cancer 2004;101:1623–31.

[11] Onishi H, Kuriyama K, Komiyama T, Tanaka S, Sano M, Marino K, et al. Clinical outcomes of stereotactic radiotherapy for stage I non-small cell lung cancer using a novel irradiation technique: patient self-controlled breath-hold and beam switching using a combination of linear accelerator and CT scanner. Lung Cancer 2004;45:45–55.

[12] Timmerman R, Papiez L, McGarry R, Likes L, DesRosiers C, Frost F, et al. Extracranial stereotactic radioablation: results of a phase I study in medically inoperable stage I non-small cell lung cancer. Chest 2003;124: 1946–55.

[13] Uematsu M, Shioda A, Tahara K, Fukui T, Yamamoto F, Tsumatori G, et al. Focal, high dose, and fractionated modified stereotactic radiation therapy for lung carcinoma patients. Cancer 1998;82:1062–70.

[14] Uematsu M, Shioda A, Suda A, Fukui T, Ozeki Y, Hama Y, et al. Computed tomography-guided frameless stereotactic radiotherapy for stage I non-small cell lung cancer: a 5-year experience. Int J Radiat Oncol Biol Phys 2001;51:666–70.

[15] Wulf J, Haedinger U, Oppitz U, Thiele W, Mueller G, Flentje M. Stereotactic radiotherapy for primary lung cancer and pulmonary metastases: a non-invasive treatment approach in medically inoperable patients. Int J Radiat Oncol Biol Phys 2004;60:186–96.

[16] Wulf J, Baier K, Mueller G, Fletje MP. Dose–response in stereotactic irradiation of lung tumors. Radiother Oncol 2005;77:83–7.

[17] Zimmermann FB, Geinitz H, Schill S, Grosu A, Schratzenstaller U, Molls M, et al. Stereotactic hypofractionated radiation therapy for stage I non-small cell lung cancer. Lung Cancer 2005;48:107–14.

A Japan Clinical Oncology Group Trial for Stereotactic Body Radiation Therapy of Non-Small Cell Lung Cancer

Masahiro Hiraoka, MD, PhD, and Satoshi Ishikura, MD, PhD†*

Stereotactic body radiation therapy (SBRT) is a new treatment modality. To confirm the safety and efficacy, the Radiation Therapy Study Group of the Japan Clinical Oncology Group (JCOG) has started a phase II study of SBRT for stage IA non-small cell lung cancer (JCOG 0403). This study is ongoing with a strict quality control and quality assurance program, and the results will indicate whether a future phase III trial comparing SBRT with surgery is warranted. In addition, international collaboration will be critical to establish the role of SBRT in the treatment of lung cancer.

Key Words: Stage I non-small cell lung cancer, Stereotactic body radiation therapy, Clinical trial.

(*J Thorac Oncol.* 2007;2: Suppl 3, S115–S117)

Lung cancer is the leading cause of cancer-related death for men and the second for women in Japan. During 2003, approximately 57,000 patients died of lung and bronchus cancer,[1] and the number is not decreasing. Because of the application of spiral computed tomography (CT) for lung cancer screening, the number of patients with early-stage non-small cell lung cancer (NSCLC) has increased recently. The number of elderly patients who are not suitable for surgery has also increased. Although surgery is the accepted standard of care for stage I NSCLC, conventional radiotherapy has been applied for these frail patients with inferior survival compared with surgery.

Stereotactic body radiation therapy (SBRT) is a new treatment modality based on the same principles and the great success of stereotactic radiosurgery/radiotherapy for intracranial tumors. The success and high local control with minimal toxicity have drawn much interest in the application of this treatment for extracranial regions, and there are several single institutional retrospective reports.[2–8]

*Department of Radiation Oncology and Image-Applied Therapy, Kyoto University Graduate School of Medicine, Kyoto; †Outreach Radiation Oncology and Physics, Center for Cancer Control and Information, National Cancer Center, Tokyo, Japan.

Disclosure: The authors declare no conflict of interest.

Address for correspondence: Masahiro Hiraoka, MD, PhD, Department of Radiation Oncology and Image-Applied Therapy, Kyoto University Graduate School of Medicine, 54 Shogoin Kawaharacho, Sakyo-ku, Kyoto 606-8507, Japan. E-mail: hiraok@kuhp.kyoto-u.ac.jp

ISSN: 1556-0864/07/0207-0115

Although there is no large-scale prospective trial confirming the safety and efficacy of SBRT for early-stage NSCLC, it has been widely used in Japan. Onishi et al. have reported the results of a multicenter retrospective survey.[9] Data from 245 patients from 13 institutions were analyzed. There was a large variation in the dose schedule used (18-75 Gy in 1-22 fractions), and they used a biologically effective dose (BED) to account for it. With a median follow-up of 24 months, local recurrence occurred in 8% for BED $\geq$100 Gy and 26% for BED $<$100 Gy. The 3-year overall survival for medically operable patients treated with BED $\geq$100 Gy was 88%. Onishi et al. claimed that SBRT may achieve equivalent local control and survival compared with surgery; however, as in any retrospective study, it has many inherent limitations: relatively short follow-up with many censored cases, which leads to the overestimation of local control and survival; patient selection because SBRT is more often applied at a higher dose to a peripheral lesion that has favorable outcome compared with a central lesion; migration between operable and inoperable because advanced age was considered to be inoperable, which may lead to Will Rogers phenomenon; and a limited number of patients in subgroup analyses.

Therefore, we decided to develop a prospective trial to evaluate the safety and efficacy of SBRT for stage IA NSCLC.

JAPAN CLINICAL ONCOLOGY GROUP TRIAL OF SBRT FOR STAGE IA NSCLC

The Japan Clinical Oncology Group (JCOG) 0403 is a single-arm phase II study. This study was planned to determine whether SBRT is superior to conventional radiotherapy for medically inoperable patients and to explore whether SBRT can achieve survival comparable to that with surgery for operable patients with clinical stage IA NSCLC. The primary endpoint is 3-year overall survival, and the planned accrual was 100 inoperable and 65 operable patients. Local progression-free survival, patterns of failure, and toxicity were included as secondary endpoints.

Eligibility criteria included previously untreated patients with pathologically proven NSCLC; age $\geq$20 years; performance status (based on Eastern Cooperative Oncology Group scale) 0 to 2; $PaO_2 \geq 60$ torr; and $FEV_{1.0} \geq 700$ ml. All patients signed written informed consent in accordance with each institutional review board.

Patients were stratified into two groups after consultation with an experienced thoracic surgeon: 1) operable pa-